Manuscript for DesignCon 2007, Santa Clara, CA.

DesignCon 2007

Losses Induced by Asymmetry in Differential Transmission Lines

Gustavo Blando, Sun Microsystems

Jason R. Miller, Sun Microsystems

Istvan Novak, Sun Microsystems

Abstract

Even though differential transmission lines are normally modeled and analyzed as perfectly balanced structures, during the fabrication process asymmetries are observed that in some cases substantially increase the differential loss profile. In this paper, we'll examine this added loss due to nonuniformities in the dielectric material and show examples of how this can and does happen in everyday real-world systems. The paper shows the fundamental differences in these extra losses in microstrip and stripline pairs. We'll also explore different simulation methodologies to include these effects and show how this added loss closes the eye on high-speed serial data transmission as a function of frequency.

Author(s) Biography

Gustavo Blando is a signal Integrity engineer with over 10 years of experience in the industry. Currently at Sun Microsystems he is responsible for the development of new processes and methodologies in the areas of broadband measurement, high speed modeling and system simulations. He received his M.S. from Northeastern University.

Jason Miller is currently a Staff Engineer at Sun Microsystems where he works on ASIC development, ASIC packaging, interconnect modeling and characterization, and system simulation. He received his Ph.D. in Electrical Engineering from Columbia University.

Istvan Novak is a signal-integrity senior staff engineer at Sun Microsystems, Inc. Besides signal integrity design of high-speed serial and parallel buses, he is engaged in the design and characterization of power-distribution networks and packages for Sun servers. He creates simulation models, and develops measurement techniques for power distribution. Istvan has twenty plus years of experience with high-speed digital, RF and analog circuits, and system design. He is a Fellow of IEEE for his contributions to the fields of signal-integrity, RF measurements, and simulation methodologies.

1.0 Introduction

Differential transmission lines are probably one of the most used passive interconnects for high-speed data transmission. In today's marketplace, a tendency to move away from the wide and cumbersome parallel, multi-drop busses can be clearly seen; the alternative is a shift towards simpler serial interconnect interfaces, where the speeds are much higher, usually in the GBit range, and in general the topologies are much simpler (unidirectional point-to-point).

Where before we had to worry about termination strategies, synchronous timing margin, stubs for multi-loaded busses etc., now days we find ourselves worrying more about length, material properties, via stubs, impedance discontinuities, intra- and inter-pair skew, differential transmission properties etc. Passive elements in the interconnect affect transmission line properties in different ways: via stubs produce unwanted resonances, connector interfaces add crosstalk and generate reflections, edge fingers add impedance discontinuities etc. With higher signaling speeds, many effects once considered second-order, including non-ideal differential transmission lines, are now taking on increased importance [3-4]. There is a wide-spread understanding of differential transmission-line concepts, but many of the studies assume perfectly symmetrical lines, where each side of the pair has the same physical dimensions and the same temporal propagation characteristics (i.e. delay).

There are several prior studies addressing some of these asymmetrical characteristics. [1] Derives the generalized solution for asymmetrical lines by expressing the eigenvalues of the differential system. [2] Derives the symmetric, full four-port S-parameters of a differential transmission line. More recent studies such as [4], examined the impact of the weave effect, where the two sides of the differential pair may experience different per unit length propagation delays due to differences in the material properties. [3] Provided a mathematical derivation of the asymmetrical transmission line properties using L and C elements.

In this work, we study the additional losses introduced in differential transmission lines due to asymmetries. Although asymmetries can be both physical and temporal, in this study we'll concentrate on the temporal asymmetries due to the relative difference in propagation delay caused by the weave effect. In this paper we examine the case where one side of the differential pair travels mostly on top of the glass bundle and the other side of the pair trace travels close to the resin region. The characteristics of idealized and realistic stripline and microstrip pairs are analyzed. Accurate measurements of typical system differential transmission lines are taken and correlated to simulation results. A simplified mathematical model, which includes the asymmetry effect, will be presented. Finally, time domain simulations are performed with and without temporal asymmetries to quantify the voltage and time degradation due to this effect.

2.0 Differential Transmission Line Formulation

When considering an asymmetric and inhomogeneous pair of transmission lines, the general mathematical formulation can be obtained by solving the eigenvalues as shown in [1]. However, to understand the important characteristics and features of asymmetrical and/or non-homogeneous differential pairs, a very simple lumped model can also be used, as shown in Figure 1.

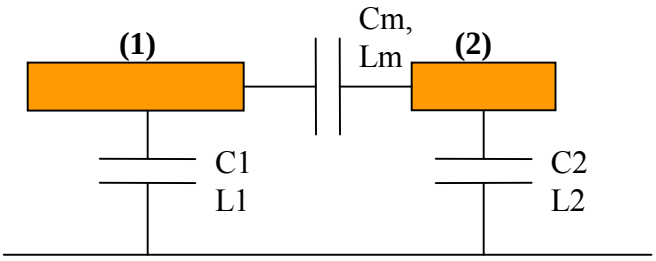

Figure 1: Lumped representation of a generic asymmetrical differential pair. For sake of simplicity, only the capacitive elements are shown.

We assume a reciprocal circuit, so that the mutual terms will reduce to one Lm and one Cm. We further assume relatively small coupling Cm << (C1, C2) and Lm << (L1, L2) as well as small asymmetry C1 ~ C2 and L1 ~ L2. With these assumptions a simple formulation can be developed. The differential mode characteristic impedances and propagation delays are calculated as shown in Equations 1 and 2. Differential mode is defined as a case when the waves have equal magnitude but opposite phases on the two lines. Similarly, common mode is defined as a case when the waves have equal magnitude and same phase on the two lines.

(1) $$Z1d = \sqrt{\frac{L1 - Lm}{C1 + Cm}} \approx Zo1.(1 - 2Kb1)$$

Where $Zo1 = \sqrt{\frac{L1}{C1}}$ and $Kb1 = \left(\frac{Cm}{C1} + \frac{Lm}{L1}\right).\frac{1}{4}$

(2) $$tpd1\_d = \sqrt{(L1 - Lm).(C1 + Cm)} \approx tpd1.(1 - 2.Kf1)$$

Where $tpd1 = \sqrt{L1.C1}$ and $Kf1 = \left(\frac{Cm}{C1} - \frac{Lm}{L1}\right).\frac{1}{4}$

The above parameters are valid for both forward and backward traveling waves. It's important to note that in any two-conductor structure with non-zero coupling, the differential and common mode parameters of one conductor depend on the presence and the excitation of the other. Equations 3 and 4 show the summary of the differential parameters, and Equations 5 and 6 show the same for the common mode parameters. In this formulation we are considering the generic case where each conductor could have different geometry and could be surrounded with different dielectric materials.

(3) $$Z1d \approx Zo1.(1 - 2.Kb1), \quad Z2d \approx Zo2.(1 - 2.Kb2)$$

(4) $$tpd1\_d \approx tpd1.(1 - 2.Kf1), \quad tpd2\_d \approx tpd2.(1 - 2.Kf2)$$

(5) $Z1c \approx Zo1.(1+2.Kb1)$, $Z2c \approx Zo2.(1+2.Kb2)$

(6) $tpd1\_c \approx tpd1.(1+2.Kf1)$, $tpd2\_c \approx tpd2.(1+2.Kf2)$

In case of an asymmetrical transmission-line pair, these parameters need to be calculated at a generic location and a generic time point. The excitation balance may be changed as the two traces may have different attenuations and propagation delays. This will result in a time and location-dependent differential and common-mode impedance and delay parameters.

A two-conductor asymmetrical transmission line will have two sets of modal propagation velocities, with different values for the two lines.

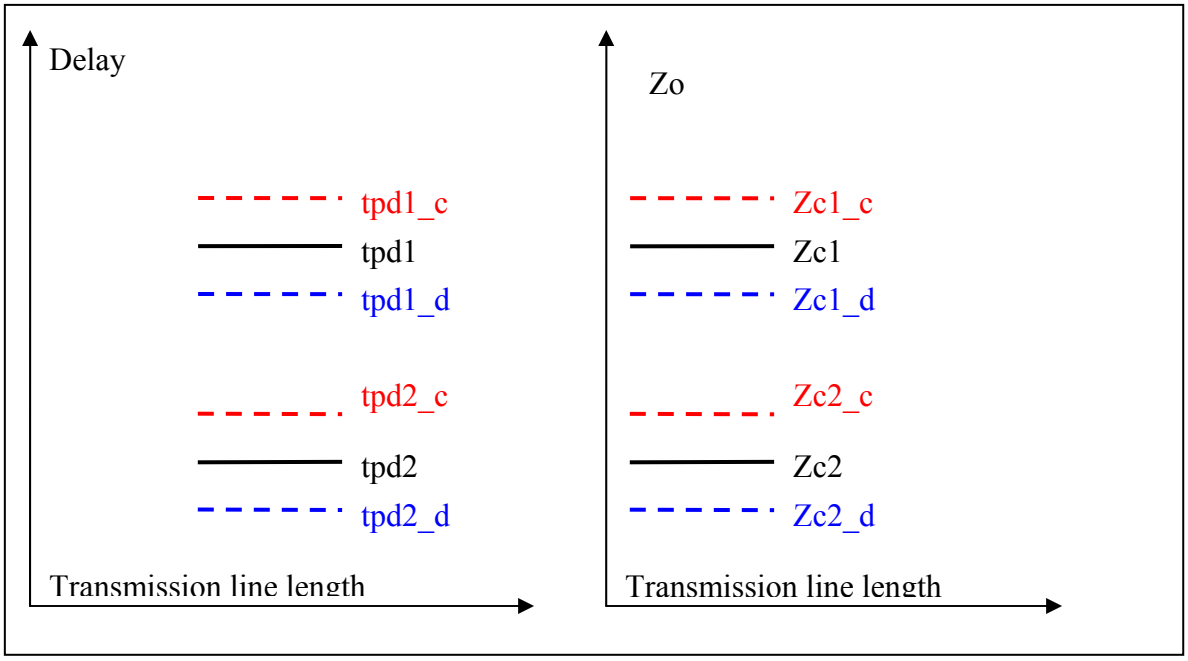

Figure 2: Graphical representation of the differential and common-mode parameters of a general asymmetrical two-conductor pair.

Figure 2 is a graphical representation of the general asymmetrical and non-homogeneous case, where all the propagation and impedance parameters are different. This graphical representation is at an arbitrary location and time on the coupled pair.

On a generic asymmetric line, the two composite waves on the two lines may have different speeds (temporal asymmetry) and therefore each line periodically will experience differential and common mode excitations and everything in between, changing the propagation delays and impedances within the dashed limits in Figure 2.

In addition to the generic solution, there are specific simpler cases. In the following sections we'll show the measurements for several kinds of lines and we'll explain the modal behavior using the graphical representation for each individual case.

3.0 Test Board Measurements

Frequency-domain measurements were made on different types of differential transmission lines in order to understand their behavior in terms of asymmetry.

A test coupon was created with five different transmission lines per layer and six routing layers. Figure 3 shows the board layout and a picture of the traces including the wafer probe used for the measurements. In order to measure the stripline, the board was milled down all the way to the stripline area exposing the copper surfaces. Differential 500 μm GSSG wafer probes were used at each end of the differential lines, and measurements were taken using an Agilent 4-port VNA with a linear sweep ranging from 300 KHz to 20 GHz with 1601 points. The measurement setup was calibrated at the end of the wafer probe tips using a SOLT wafer calibration substrate. A large number of the differential pairs in the five different boards were measured.

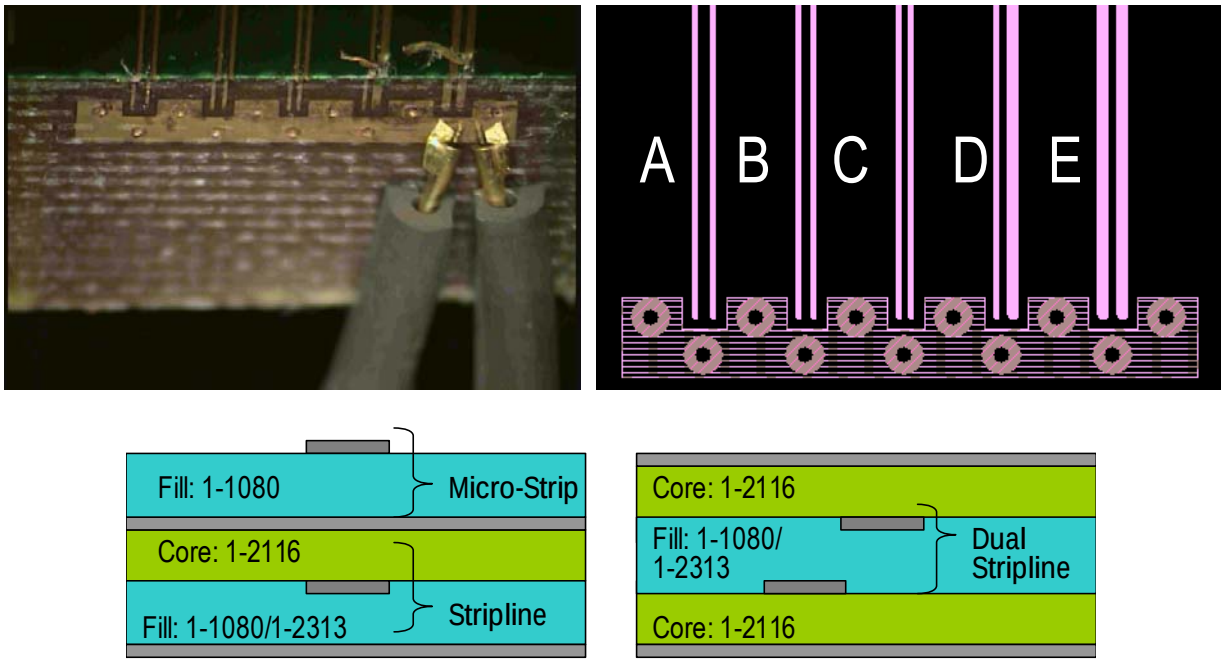

Figure 3: Differential transmission lines layout (top right) and picture of the milled-down board including the wafer probe used for the measurement (top left) as well as microstrip, stripline and dual-stripline construction sketches.

All the differential pairs were straight 14-inch long traces and they varied in trace widths and air gap as follows:

A: Line width = 4 mils, Air-gap = 8 mils
B: Line width = 4 mils, Air-gap = 6 mils
C: Line width = 4 mils, Air-gap = 4 mils
D: Line width = 4 mils/8mils, Air-gap = 4 mils
E: Line width = 8 mils, Air-gap = 4 mils

These five pairs were routed on four inner stripline layers, and on both the top and bottom microstrip layers. Case B targeted approximately 100-ohm differential impedance.

All the measurements and post-processing assumed the port ordering shown in Figure 4. The S-parameter measurements were made in a 50-ohm environment (Z_L = 50 ohm). For post-processing, the full S-parameter matrix was converted to its mixed-mode matrix counterpart with the port ordering as shown on Figure 5. In case of symmetrical lines, mode1 and mode2 represent the differential and common propagation modes, respectively.

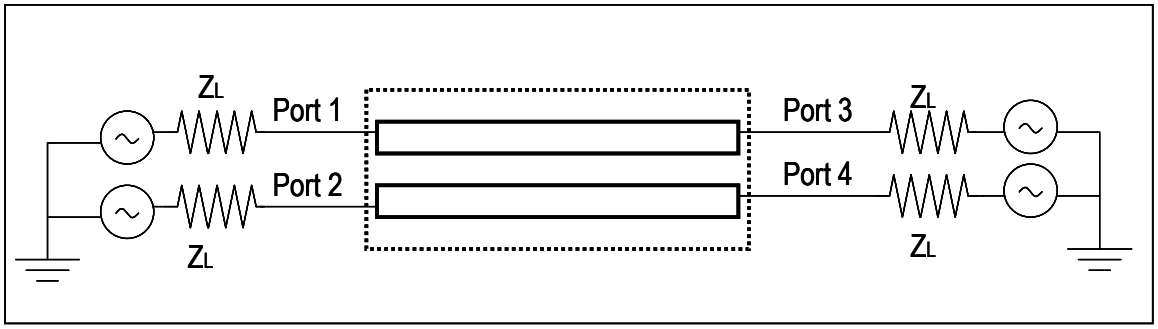

Figure 4: S-parameter port ordering.

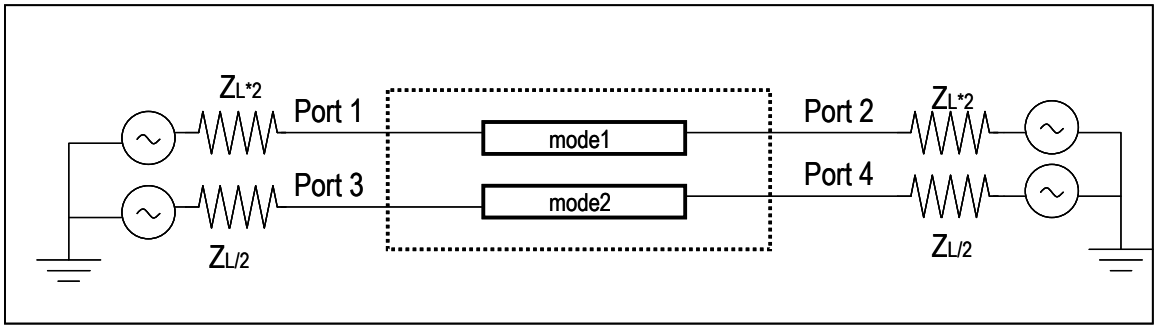

Figure 5: Mixed-mode S-parameter ordering.

It is important to clarify some of the terminology before moving forward. When referring to a *symmetrical structure*, we mean that the two lines are electrically the same, namely each side of the differential pair will have the exact same cross-sectional dimensions and will be surrounded locally by the same type or types of dielectric materials. We call a structure *homogeneous* when the cross section carrying the wave is filled with the same dielectric material. Furthermore we assume that the structure is *uniform*, which means the electrical parameters do not depend on the location along the length of coupled pair. Though in practical PCB structures uniformity is probably the hardest to maintain on a micro level, for the purposes of modeling we can assume that any non-uniform pair can be approximated with a number of cascaded uniform sections.

A microstrip pair, when above and below the traces the dielectric constant is different, is non homogeneous, regardless of the possible symmetry of the structure. If furthermore the two traces have different geometry, and/or due to spatial differences in the dielectric material (like glass-weave effect) the dielectric constant is different around the two traces, the pair will be non homogeneous *and* asymmetrical. An ideal stripline pair with the same uniform dielectric material above and below the traces is a homogeneous structure. If the geometries of the traces are identical, it is also symmetrical.

If the traces have different geometries, the structure becomes asymmetrical. If the dielectric material is locally different around the two traces, the structure becomes non homogeneous and asymmetrical.

Figure 6 shows some of the important variants in terms of construction, asymmetry and homogeneity. Note that the middle two sketches in Figure 6 are labeled as symmetrical, referring to the case when the glass-weave effect creates locally varying dielectric constants, but because the changes are assumed to be symmetrical around the two traces, the structure stays electrically symmetrical, but non-homogenous. This assumes though that the geometries of the two traces are identical. If the traces have different geometries, and/or –as shown on the bottom two sketches in Figure 6 - the glass-bundle positions are asymmetrical with respect to the traces, the structure becomes asymmetrical.

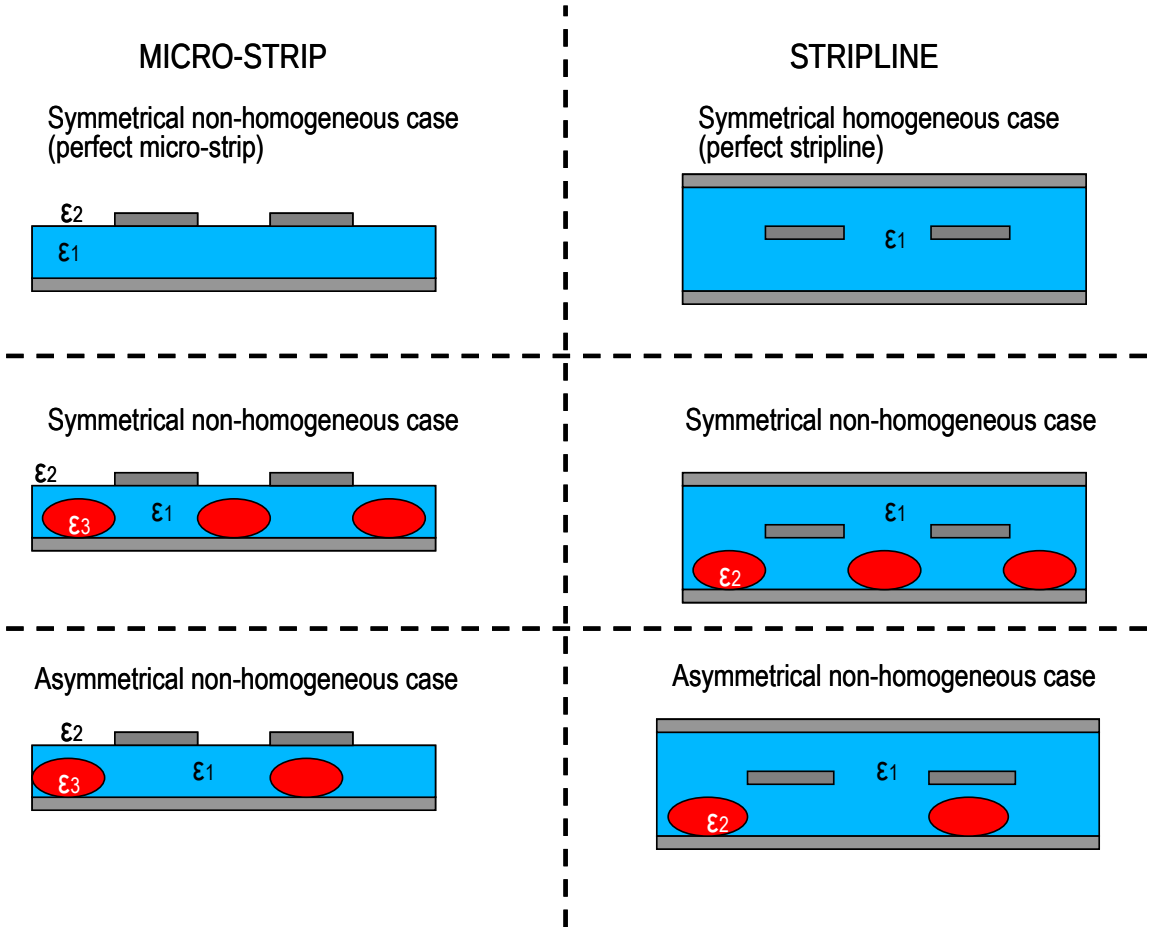

Figure 6: Differential transmission line groupings.

3.1 Microstrip Case

A microstrip pair with the same geometry of the traces and uniform dielectric between the traces and the plane represents the inhomogeneous, symmetrical case from the top left sketch of Figure 6. Figure 7 shows the measured S13 and S24 insertion loss and group delay on such a pair. As can be seen in the figure, for both sides of the differential pair, there are multiple frequencies with dips in the stand-alone insertion loss and group delay. On the other hand, the mixed-mode S-parameter insertion loss, as shown in Figure 8 (left) shows a straight profile of the insertion loss without any dip. At the same time, the extracted modal group delays show a rather large difference between the propagation modes.

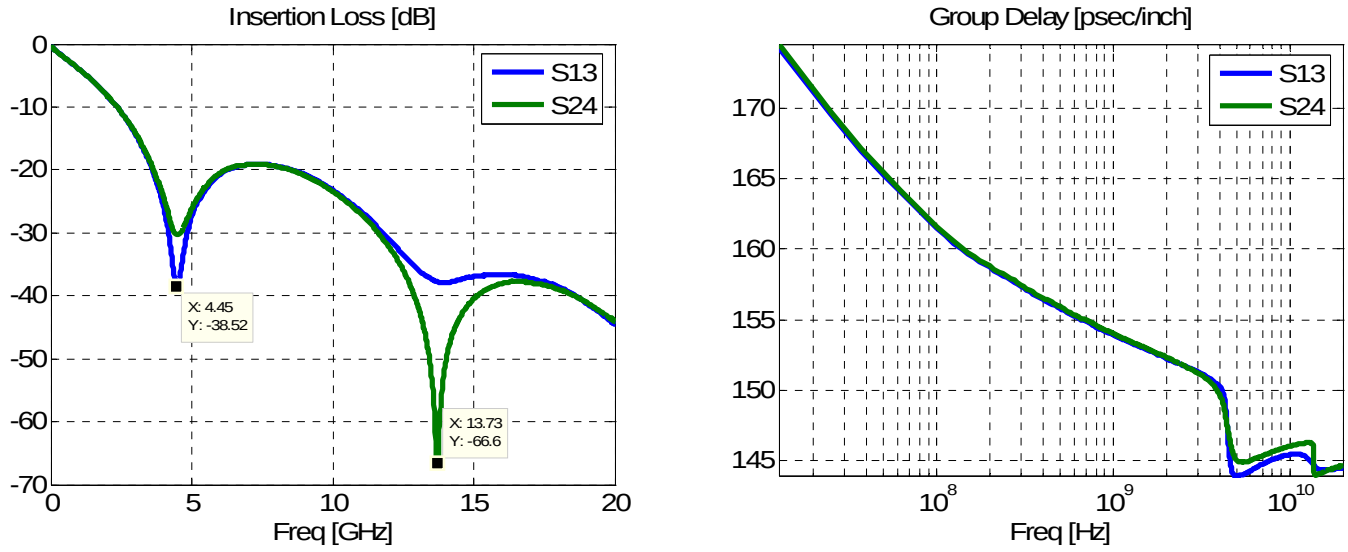

Figure 7: Microstrip insertion loss (left) and group delay (right).

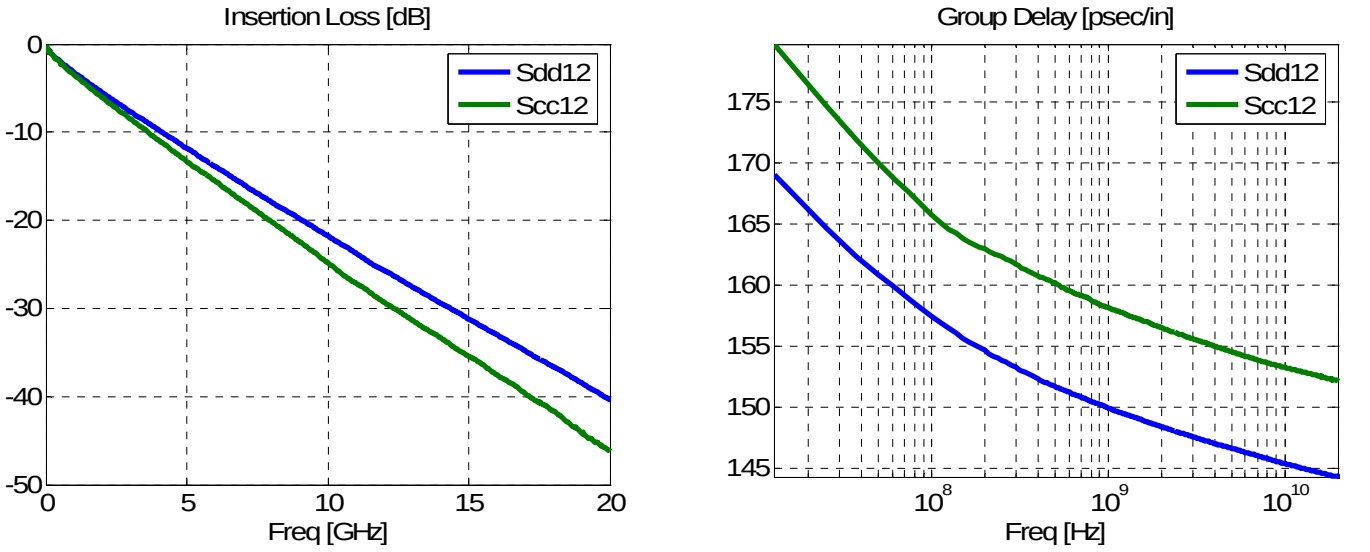

Figure 8: Microstrip mixed-mode insertion loss (left) and mixed-mode group delay (right).

In order to understand this structure, let's first take a step back and remember how this structure was measured. The VNA measurement procedure injects a signal in one port and measures the response on the all of the ports. Even though only one of the traces was excited at a time, both traces and all four nodes were terminated in 50 ohms. In this case, since we are measuring a differential transmission line, we can help our understanding by algebraically decomposing the VNA single-ended excitation into two components, differential and common mode, as follows:

$$vd = v1 - v2, \quad vc = \frac{v1 + v2}{2}$$

$$v1 = vc + vd/2 \tag{7}$$

$$v2 = vc - vd/2$$

Vc and Vd are defined as the common mode and differential mode excitation, respectively. This assignment of source voltages restores zero source voltage for the unexcited trace. By performing this transformation and assuming the transmission lines are excited as shown in Figure 9, the circuit can be analyzed by first applying the differential excitation, then the common mode and finally using superposition to reconstruct the nodal voltages at the ports (i.e., P1, P2, P3, and P4).

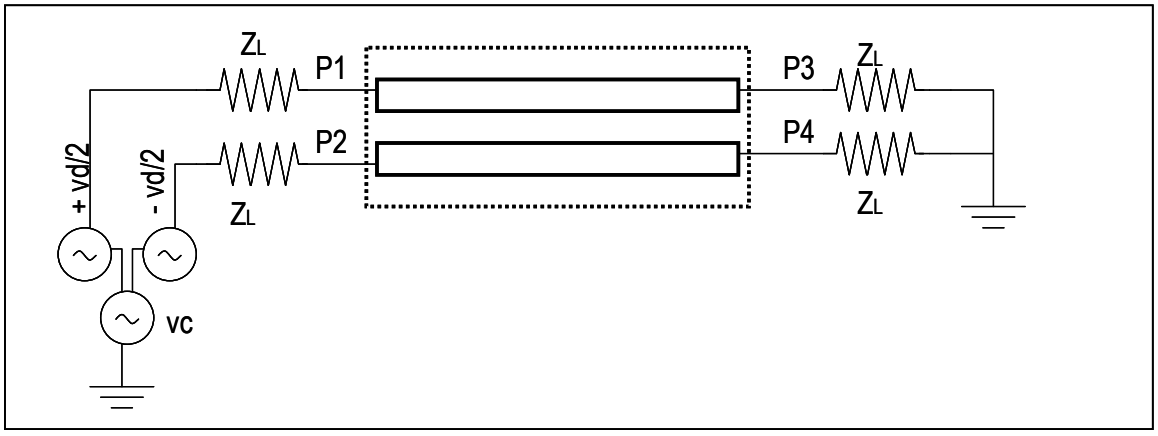

Figure 9: Differential and common-mode excitation.

For a symmetrical structure, when we apply a differential or common mode input, we excite only the odd or even transmission line modal propagation, respectively. Referencing Figure 8, this means for example, that the odd mode will propagate at 150 ps/in and the even mode will propagate at 157 ps/in, based on the mixed-mode group delays at 1 GHz. These two modes propagate at different speeds and can be visualized with phasors as shown in Figure 10. When exciting the differential transmission line structure as the VNA does, one port at a time, both modes get excited and they propagate at different speeds through the structure.

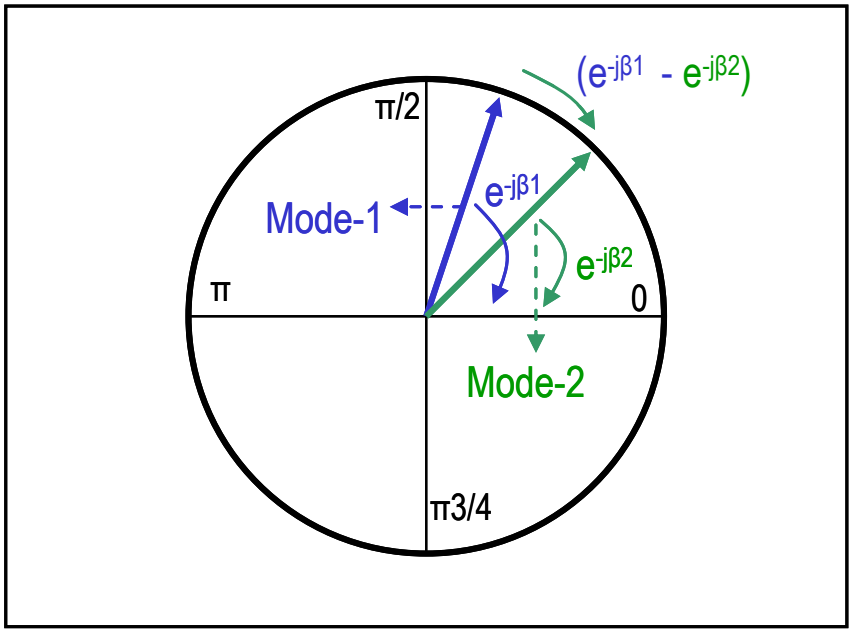

Figure 10: Phasor representation of the modal velocities.

In this diagram, each mode is represented by a vector, each rotating with a different velocity. At any point on the transmission line, we can calculate the nodal voltages using Equation 7 for these two modal propagating voltages.

As these two independent modes propagate along the line, there are locations and frequencies, where the phase difference will reach π, 3π, 5π. At those frequencies and locations, by superposition, we'll observe a cancellation of the nodal voltages. By computing the modal propagation delay difference, multiplying by the trace length and calculating the mean of the result as a general approximation for all frequencies, we get a delta propagation delay of 111 ps for the entire 14" length, as shown in Figure 11.

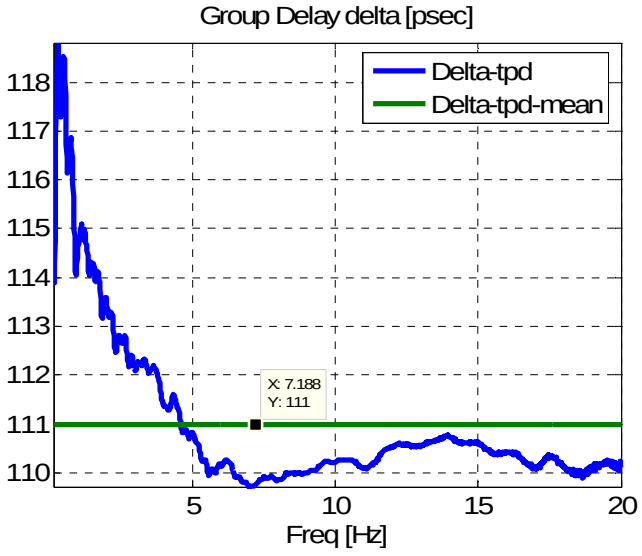

Figure 11: Microstrip modal propagation delay difference.

Using the delta delay approximation of Figure 11, the cancellation frequencies (fr), can be calculated by the following simple approximation:

$$(8) \qquad fr = \frac{2n+1}{2.delta\_tpd}$$

For n = 0 and n = 1 the dips will occur at 4.5 GHz and 13.5 GHz, respectively, which are the locations of the frequency dips in Figure 7.

Now, the next question to answer is why the differential and common-mode insertion losses do not exhibit these frequency dips. This can be very simply explained by the fact that in the presence of a symmetrical differential transmission line, a differential input excites only one of the modes. We assumed light coupling and matched terminations, therefore mode conversion can be neglected. Since the other mode is not present, cancellation does not occur. This is equivalent to a single rotating phasor in Figure 10.

By using the graphical representation developed in Figure 2, Figure 12 shows that for a symmetrical structure tpd1 = tpd2. Due to the assumed symmetry, Kf1 is equal to Kf2, but because the structure is non-homogeneous, they are not zero. As observed in Equations 3 through 6, this will result in two modes traveling at different speeds. We also note that the more we separate these conductors, the weaker becomes the coupling, and the modal propagation delays will get closer to the center. At the extreme case, with no coupling, tpd_c and tpd_d will asymptotically blend into tpd as is the case for a single-ended transmission line.

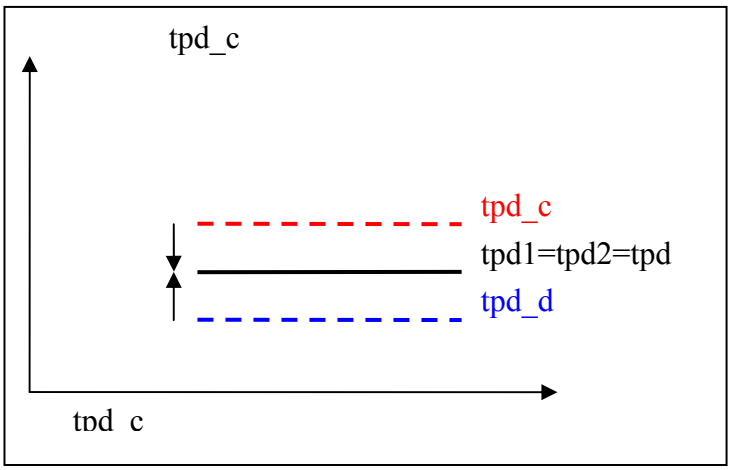

Figure 12: Graphical representation of the propagation delays of an ideal microstrip pair.

To summarize, there are a few important points to remember:

- The frequency dips on the S-parameters are due to the differences in the modal propagation delays.
- The modal propagation-delay difference in an inhomogeneous medium is due to the coupling; as the coupling tends towards zero, the difference in propagation delay also tends towards zero.
- When exciting a symmetrical differential transmission line with a differential or common mode excitation, only one mode or the other will be present in the structure.

3.2 Homogeneous Stripline

The homogeneous stripline is probably the most frequently used model for differential signaling, and gives a very good approximation for most real applications. From our analysis point of view, it's probably the least interesting, since there are not many distinct features to discuss.

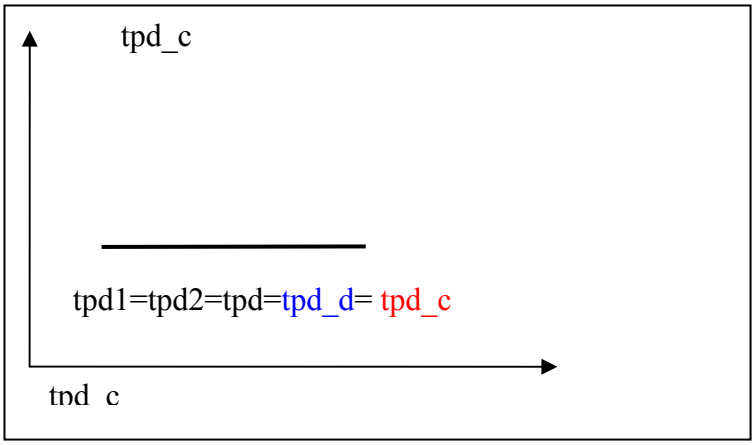

Figure 13: Graphical representation of the symmetrical stripline propagation case.

Figure 13 shows the graphical representation of the delays of a perfectly symmetrical homogeneous stripline case, where all the velocities are the same. Here, regardless of the kind of the excitation, single ended, common mode or differential, no nulls will be observed, since all the propagation speeds are the identical.

Figure 14 shows the measured S13 and S24 insertion losses and group delays on a symmetrical stripline pair. In this case, there are no frequency dips as observed on microstrips, because of the homogeneity of the material. By looking at the mixed mode S-parameters, again due to the symmetry of the structure, the insertion loss profile looks very smooth and well behaved. Also note that the data shows little modal propagation delay difference over frequency.

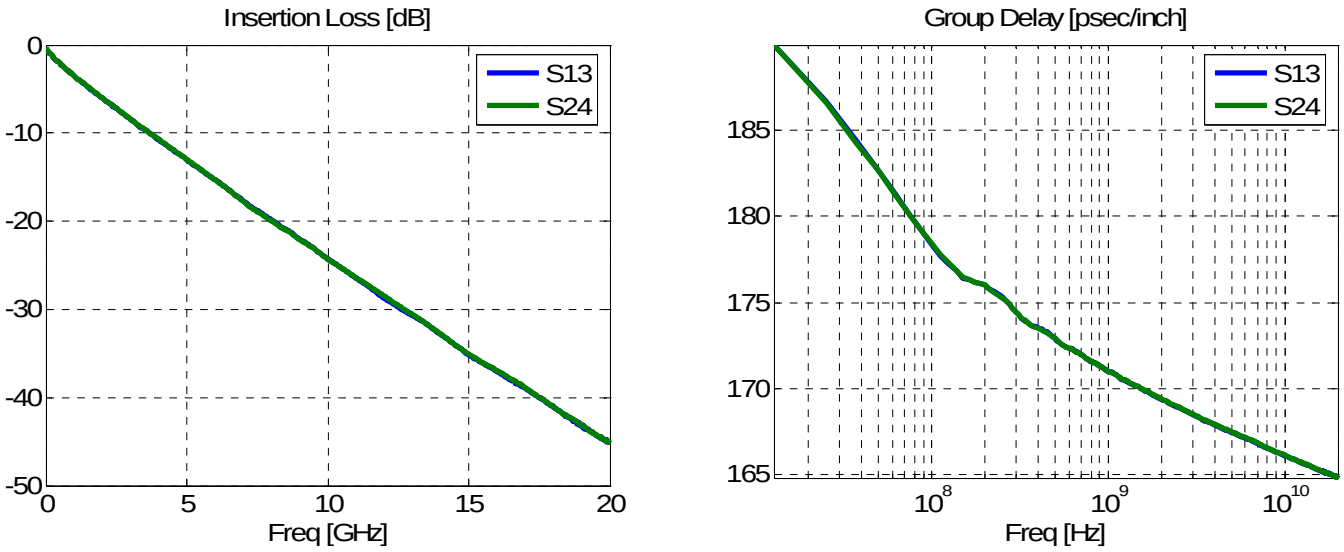

Figure 14: Stand-alone insertion loss (left) and group delay (right) of a symmetrical and homogeneous stripline pair.

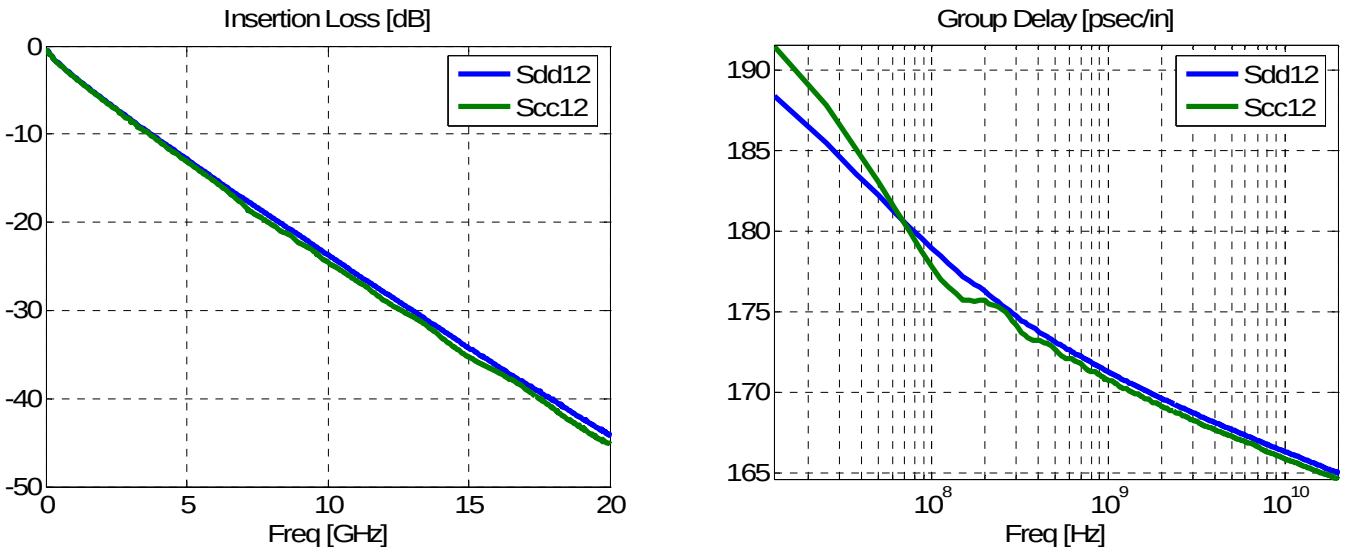

Figure 15: Mixed-mode insertion loss (left) and mixed-mode group delay (right) of the symmetrical and homogeneous stripline pair.

This is the behavior we expect in stripline designs. Unfortunately, due to unavoidable fabrication and material imperfections, practical cases may deviate from this ideal case. If that happens, the homogeneity or temporal symmetry assumption need to be removed and again we start seeing frequency dips, but now it happens on stripline (as shown below).

3.3 The Glass-Weave Effect: The "almost homogeneous" Stripline Case

From the previous discussion, we've gained an understanding of the mechanism that produces the extra attenuation for differential propagation. In this section, we examine what is commonly referred to as the glass-weave effect, defined as the skew observed between two lines when one of the lines runs mostly over the glass bundle while the other runs mostly over the resin, both material having different dielectric characteristics. [4] made a study of this effect and showed that glass weave effect could add, in some cases, up to 7ps/inch skew between two legs of a differential pair.

To capture this temporal asymmetry due to the glass-weave effect, is not a trivial matter. Let us consider the following:

- The manufacturer does not guarantee, nor specify the orientation of the glass bundles on the panel, it could be parallel, or maybe with some small angle.
- In order to see a pronounced effect, one of the traces should run on top of the bundle for most of its lengths while the other should run on top of the resin. Since the angle of the glass weave bundle is not specified, the longer the net, the more probability of propagation-delay averaging
- In order to isolate the effect, this measurement needs to be performed on a "perfect" stripline, meaning a trace pair that does not have any bends or vias. The implication of this, apart that the line needs to be straight, is that direct measurement access is needed on an inner stripline for wafer probes.

Figure 16 shows the measured S13 and S24 insertion loss and group delay on a stripline pair showing the glass-weave effect. From this Figure something rather interesting can be observed. First, the insertion loss profile is smooth not showing any dips, and furthermore, the S13 and S24 group delays are different, meaning there is a difference in the propagation delays between each side of the differential pair. This case behaves very differently from both a microstrip and a homogeneous and symmetrical stripline pair.

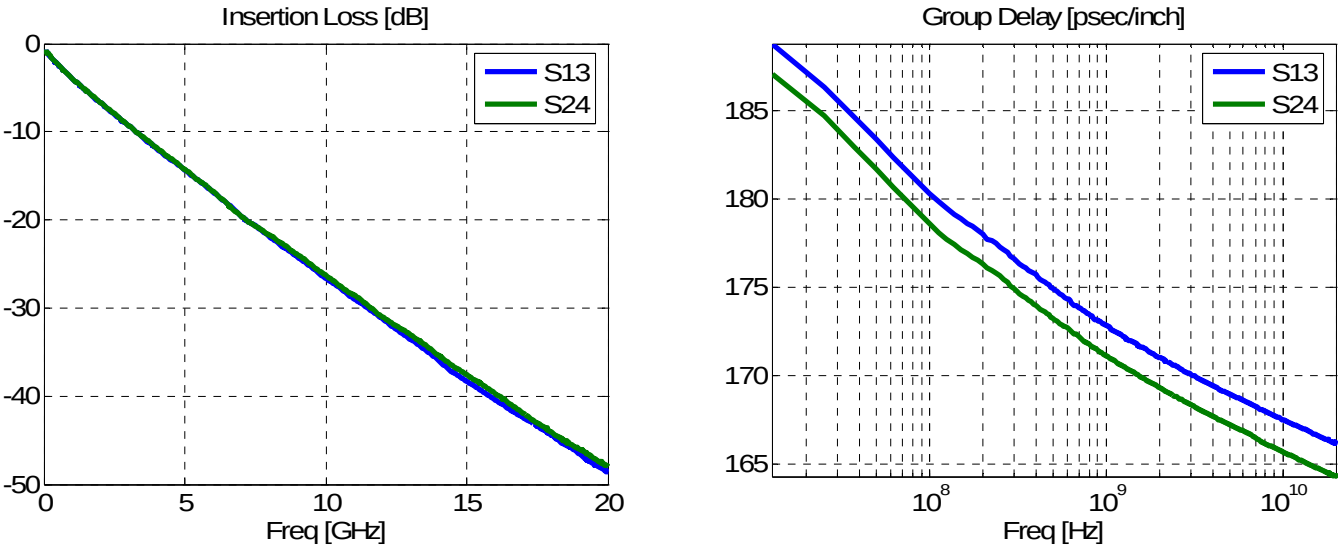

Figure 16: Insertion loss (left) and mixed-mode group delay (right) of a non-homogeneous and asymmetrical stripline pair.

When we convert this matrix to its mixed-mode S-parameter counterpart, some new and interesting features start to show up.

Figure 17 plots the mixed-mode insertion loss and mixed-mode propagation delays. The mixed mode insertion loss has a dip at approximately 20 GHz. This dip is similar to the dip in the S13 and S24 insertion loss profiles of a non-homogeneous but symmetrical microstrip pair. In fact, what is being observed is the same effect seen on the S13 and S24 profiles on microstrips with the difference that it is now seen on the mixed-mode S-parameters, not the stand-alone S-parameters. This suggests that even though the effect is the same, the underlying reason is somewhat different. Furthermore, note that the mixed-mode propagation delays are almost the same. This behavior contrasts with the microstrip case where the modal propagation delay was very different.

The assumption for this case is that one side of the differential pair is routed closer to the glass bundle while the other is routed closer to resin. This will have the effect of changing the effective Dk around one of the traces as compared to the other and hence change its propagation delay.

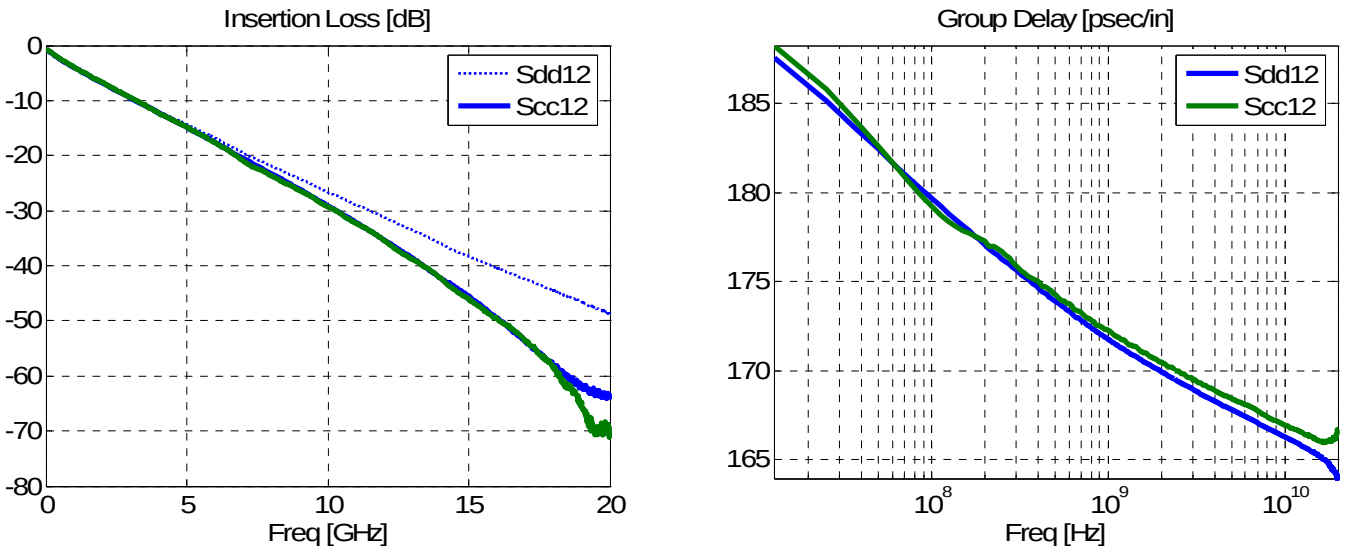

Figure 17: Mixed-mode insertion loss (left) and mixed-mode group delay (right) of a non-homogeneous and asymmetrical pair of striplines.

Referencing Figure 18, for the asymmetrical case, we can see that all the propagation delays are now distinctly different. tpd1 is different that tpd2 due to the self (L1,L2,C1,C2) parameters, and due to coupling and due to the non homogeneity of the material, tpd1/2_c is different from tpd1/2_d. In this case, if we drive a pure common-mode excitation, we notice that along the length of the transmission line there is a mode reversal. For a particular length and at a particular frequency, we will observe pure differential signal, even though the excitation is pure common mode. When we send common mode or differential signals, we'll have a continuous mode conversion and the cancellation nulls will be observed in the response.

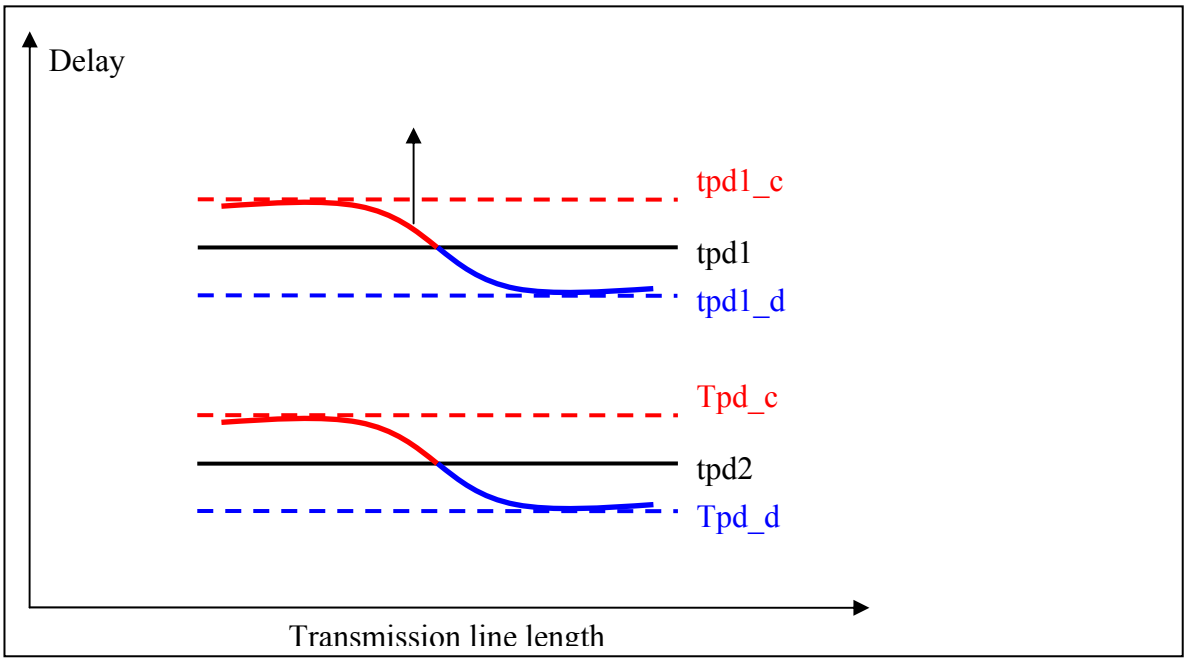

Figure 18: Graphical representation of an asymmetrical stripline propagation with a common-mode excitation.

Figure 19 shows the behavior, when the excitation is pure single ended. As previously explained, a single ended excitation can be decomposed into a differential and a common mode excitation. It can be seen that in this case we excite both modes with about equal magnitude. As the wave propagates in form of a superimposed pair of common-mode and differential-mode waves, they also continuously transform into each other. Though each mode alone would experience nulls in their transfer functions, the net result of the two superimposed modes is that we do not have cancellation in the stand-alone excitation.

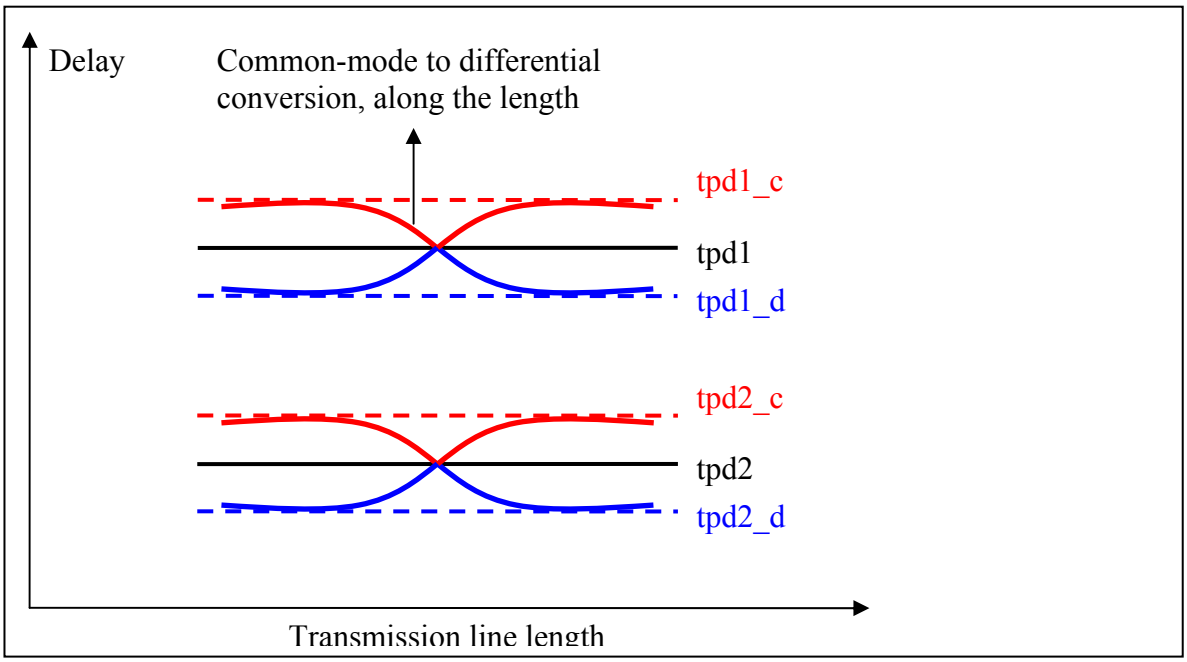

Figure 19: Graphical representation of an asymmetrical stripline propagation with a single-ended excitation.

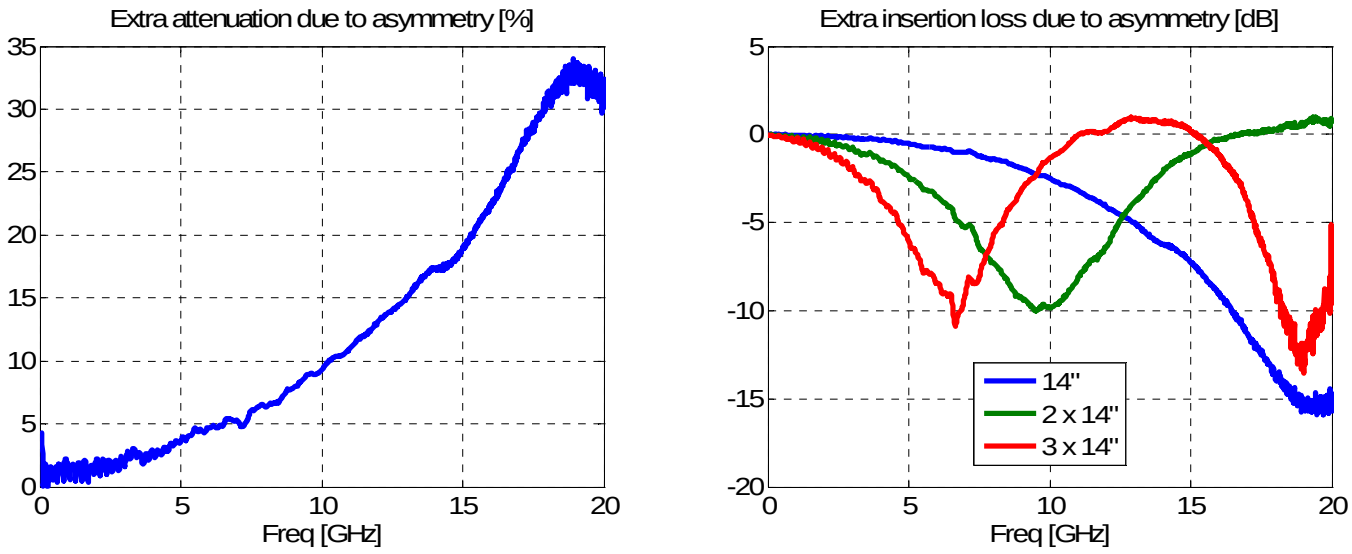

Figure 20: Plot of the extra percentage attenuation of the original data shown in Figure 17 (left) and after concatenating different numbers of unit cells (right).

Note that in differential striplines the dielectric material above and below the traces are inherently different as one comes from a core, the other from a prepreg. Unless the two dielectric constants are identical, this dielectric non-uniformity, similar to the glass-weave effect, creates a microstrip-like nonhomogenity. Therefore in a generic stripline construction we can expect attenuation dips in both the single-ended and differential transfer parameters.

Figure 20 (left) plots the extra percentage attenuation of the mixed-mode insertion loss (observed in Figure 17 (left)) with respect to the S13 baseline. By taking the original data and concatenating it by a factor of two and three, then calculating the mixed mode S-parameters and subtracting it from the S13 baseline, we obtain the plot on the right of Figure 20. As can be seen by concatenation, the 2π periodicity of the frequency dips can be clearly observed without resorting to simulations, just from the measured data.

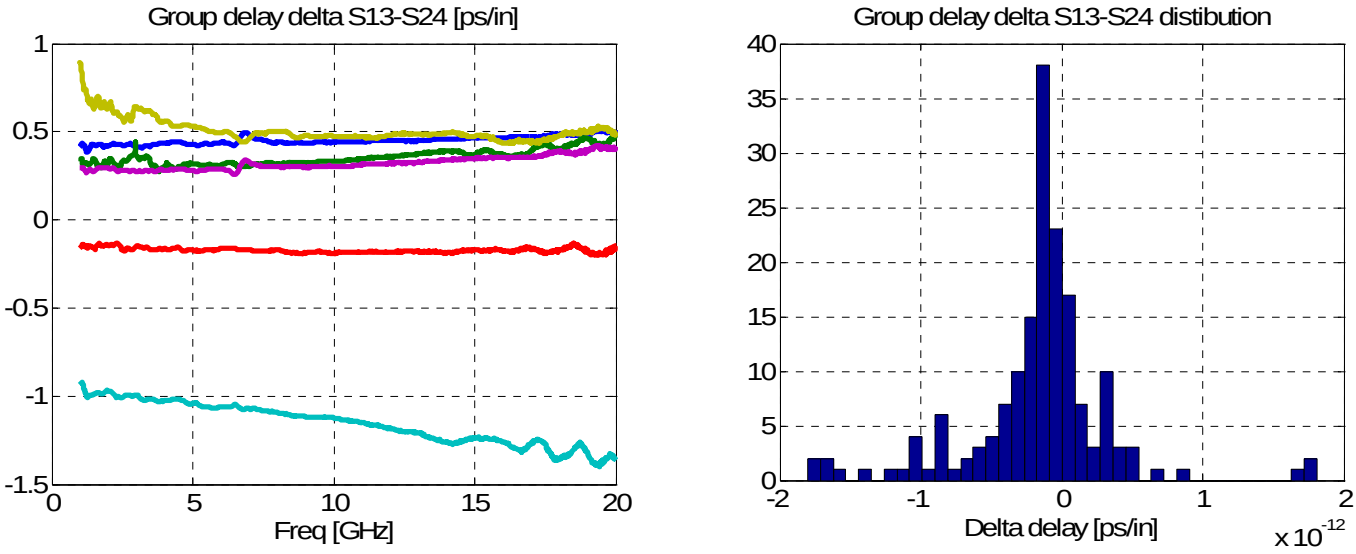

Figure 21: Difference in delay measurements (left) and distribution (right).

Figure 21 (left) plots the measured frequency dependent group delay difference between S13 and S24 from 1 GHz to 20 GHz. The mean of each frequency dependent delta delay was used to create the distribution shown in Figure 21 (right). Fitting the distribution with a Gaussian curve resulted in a mean of -0.16 ps and a standard deviation of approximately 0.5 ps.

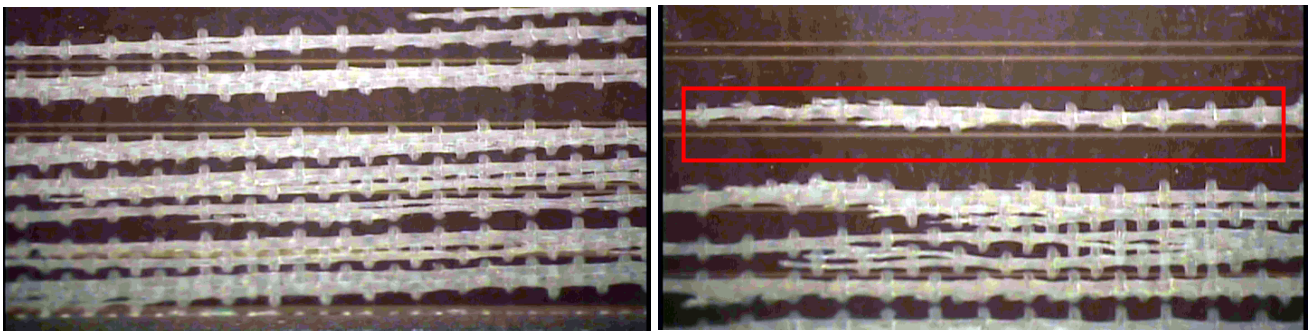

Figure 22: Photographs of the glass-weave orientation with respect to the differential pairs. Off-angle routing (left) and parallel routing (right) are shown.

After observing this rather tight distribution, some of the boards were peeled using a razor blade in an attempt to observe how the glass weave was oriented with respect to the differential transmission lines. Note that all of the measured traces were nominally parallel to the edges of the panel. Figure 22 shows photographs of the results from peeling. The vast majority of the peeled boards exhibited routing similar to Figure 22 (left) where the glass-weave is slanted with respect to the differential transmission line, explaining why most of the measured test structures showed a small amount of skew. On Figure 22 (right), the measured trace with the bigger skew is shown. In that case, it can be seen that the glass-weave bundle runs on top of one of the differential pair traces for a good portion of the overall length but not all since the weave becomes a little slanted later and starts crossing both traces. This suggests that potentially more skew could be found in some cases.

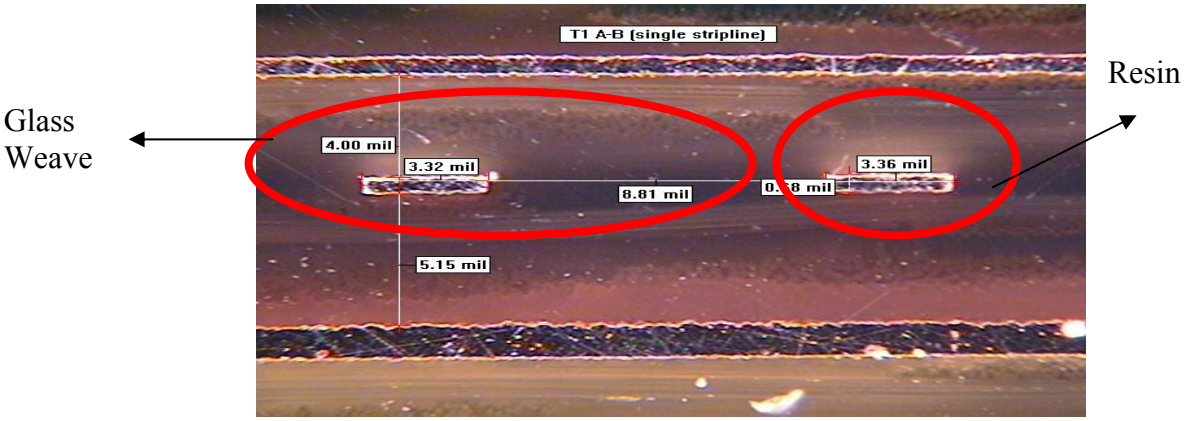

Figure 23: Cross-Section of an asymmetrical case.

Figure 23 shows a cross section of a similar board illustrating the relative location of the glass bundle and resin with respect to the signal conductors.

To summarize, it has been shown by accurate measurements that in differential stripline structures, the glass-weave effect can be observed. However, although more than 150 differential stripline pairs were measured, this behavior was measurable only in no more than three instances; the rest of the structures behaved very close to the ideal case. The worst-case difference in propagation delay encountered was approximately 1.85 ps/inch.

4.0 Simulations

We've shown in the previous section a case where there is a temporal asymmetry on a differential stripline pair. To simulate this effect, Ansoft SI2D was used to develop a very simple model. Figure 24 shows the simulated cross-section, where the asymmetry was forced by slightly changing the dielectric constants surrounding each side of the differential pair. A multi-pole Debye model was used to capture the frequency dependent dielectric material properties.

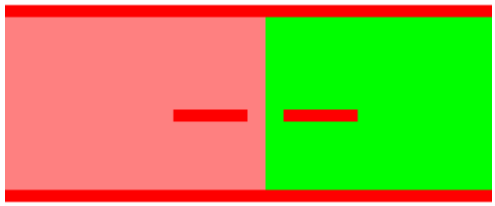

Figure 24: Simplified 2D model of the asymmetrical stripline case.

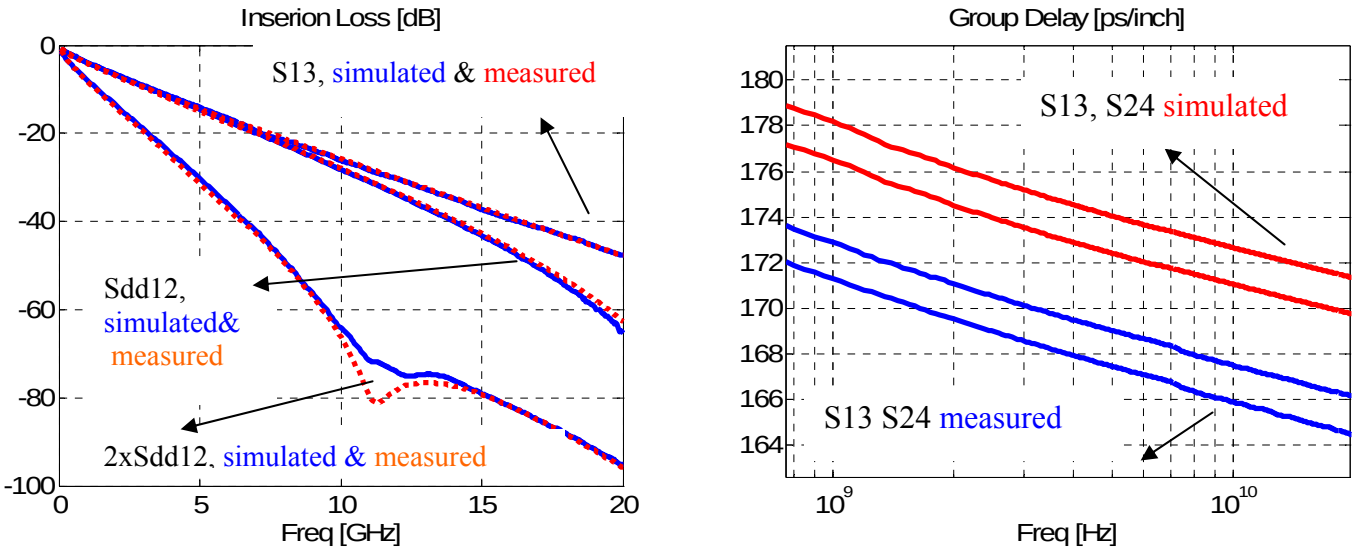

Figure 25: Simulation to measurement S-parameter correlation.

Figure 25 shows the correlation between the measured and the simulated data by the use of this simplistic model. Excellent S13 and the Sdd12 correlation is shown on Figure 25 (left). On Figure 25 (right), a correlation of the group delay is shown. It can be seen that even though the frequency dependent slope and the relative difference between the S13 and S24 group delays is very well captured, the absolute propagation delay value is different by 6 ps. This offset is attributed to differences in the absolute value of Dk; further optimizations certainly could improve the correlation.

For large backplanes, where in many cases low-loss materials and longer nets are required, the asymmetry of the weave effect will be more pronounced. From [4] it was found that in some cases the maximum propagation delay difference can be in the order of 7ps/inch. Using the simplified model introduced above, a set of simulations were performed to examine the impact of length in both the frequency and time domain. The following material and physical parameters were used:

Dielectric 1: Dk=4.0, tand=0.009 (@ 1 GHz)
Dielectric 2: Dk=4.2, tand=0.009 (@ 1 GHz)
Length: 20 inch

Two sets of simulations were performed, one where a single dielectric was used, attempting to capture the baseline case for a 20-inch interconnect, and another where the asymmetrical dielectric fill was

used. Figure 26 shows the frequency domain insertion loss characteristic of the symmetrical (i.e. baseline) versus the asymmetrical stripline. Note that on the asymmetrical case the first frequency dip is around 8 GHz. The plot on the right shows the difference between the group delays S13 versus S24 on the asymmetrical case, renormalized to ps/inch.

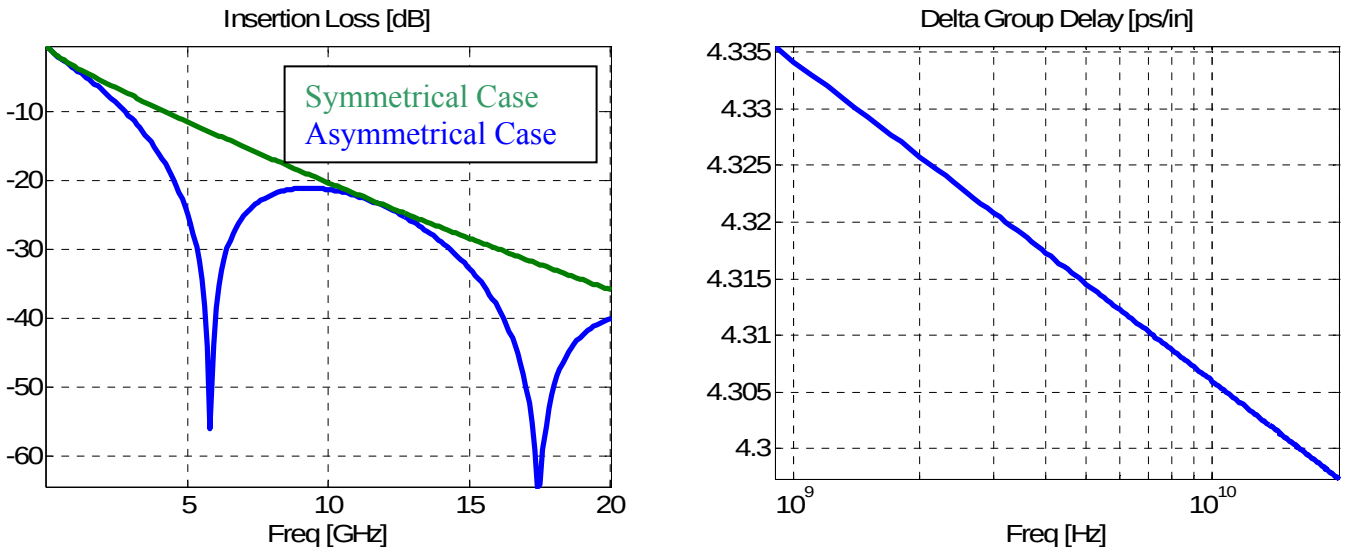

Figure 26: Frequency-domain characteristics of a simulated 20-inch symmetrical and asymmetrical differential transmission lines.

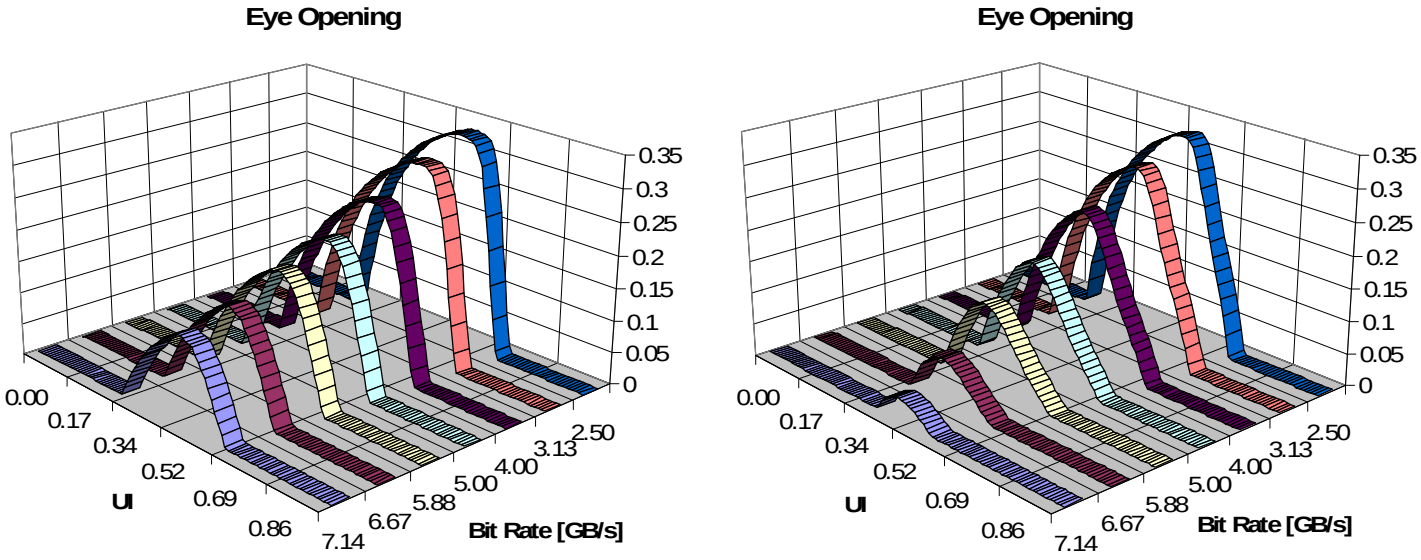

Figure 27: Eye openings for a 20-inch differential pair without asymmetry (left) and with asymmetry (right). For sake of clarity, only the upper half of the inner eye contour is shown.

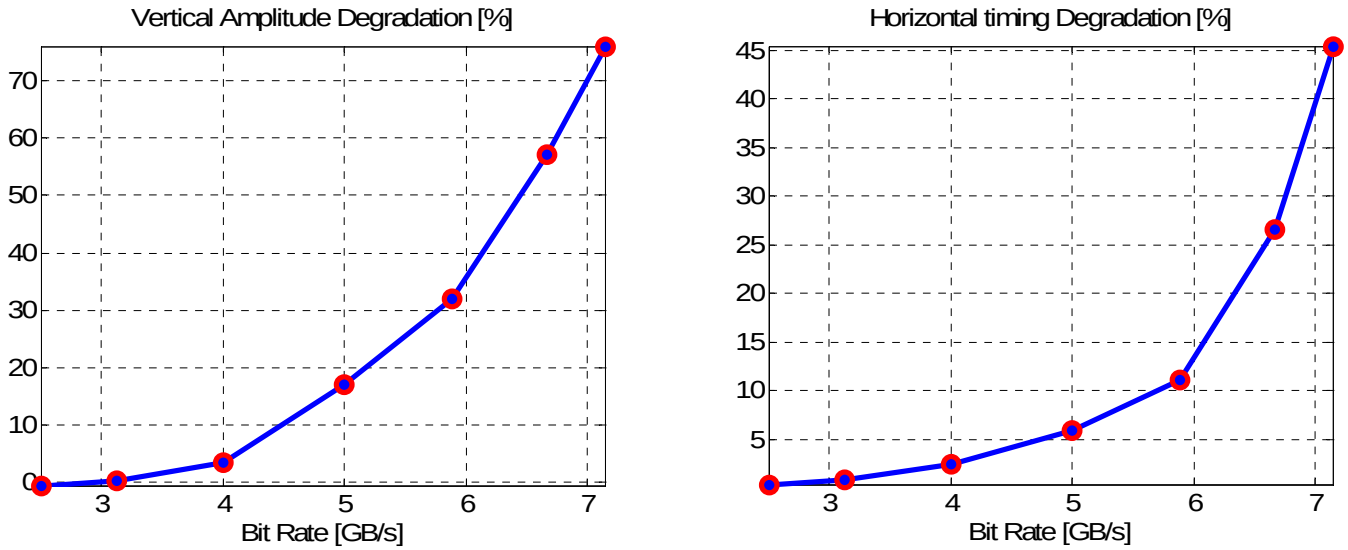

Figure 28: Additional vertical (left) and horizontal (right) degradation of eye due to differential pair asymmetry.

In order to study the impact of differential transmission line asymmetry effect and trace length on the eye diagram, several simulations were performed changing the bit rate from 2.5GB/s to approximately 8 GB/s. Eye diagrams were captured and post-processed for both the symmetrical and asymmetrical case. In Figure 27 (left), we see the eye opening as a function of bit rate for the symmetric stripline. It can be seen that even though the eye opening is shrinking due to the transmission line attenuation, we still see a reasonable eye opening at all bit rates. Figure 27 (right) plots the eye opening for the asymmetrical case. In this case, we see that at about 7 GB/s, there is almost no eye opening. At lower frequencies, there are no appreciable differences between the two cases. In essence, what we are observing in the eye opening plots is that as the data rate increases, the extra attenuation and phase distortion due to the frequency dips created by the transmission line asymmetry, significantly decreases time and voltage margin.

To further illustrate this point, Figure 28 plots the eye degradation vertical (left) and horizontal (right) percentage with respect to the baseline (i.e. symmetrical case). At the highest data rates, there is an additional 70% vertical and 45% horizontal degradation.

5.0 Conclusions

It has been shown that the asymmetry due to the glass-weave effect is seen in both microstrip and striplines in form of dips in the attenuation profiles, but not in the same way. On microstrip pairs we see the dips in the single-ended transfer functions, and it is caused primarily by the structural non-homogeneity even without the glass-weave effect. These dips come from the non-homogeneity of the cross section, regardless of local anomalies in the underlying dielectrics. In stripline pairs, on the other hand, the dielectric asymmetries show up also on the differential transfer functions, resulting from the different delays along the two traces.

In real-life differential pairs in glass-reinforced PCBs, eventually the microstrip and stripline constructions are both non-homogeneous and asymmetrical. In microstrips the structural non-homogeneity is usually stronger, resulting in nulls primarily in the stand-alone transfer functions. In striplines, usually the asymmetry dominates over non-homogeneity, resulting in dips of the differential transfer functions.

The weave effect on the high-speed signal propagation has been shown through accurate VNA measurements showing an approximate delay difference of up to 1.85 ps/in. From the more than one hundred measurements, only two cases were found with this extreme skew. By peeling the PCB structures, it was shown that the less-than-expected impact of the glass-weave effect can be attributed to the randomness of the glass bundles: on longer traces the dielectric asymmetry tends to cancel.

A simple simulation model was created that can be used to simulate the glass-weave effect in both microstrip and stripline pairs. Time domain simulations were performed showing the eye degradation with typical backplane geometries.

The unexpected increase of the propagation delay differences due to the weave effect could pose a real problem to systems since this effect depends not only on the dielectric asymmetry but also on the transmission-line length: longer traces result in lower frequency of the attenuation dip. Mitigation of this effect could be achieved by routing traces at randomized angles.

References

[1] Vijai K. Tripathi, "Asymmetric Coupled Transmission Lines in an Inhomogeneous Medium" IEEE Transactions on Microwave Theory and Techniques, VOL. MTT-23, No. 9, September 1975.
[2] L. S. Napoli and J. J. Hughes, “Characteristics of Coupled Microstrip Lines”, RCA Review, September 1970.
[3] Stephen B. Smith, “Theory and Measurement of Unbalanced Differential-Mode Transmission Lines”, Proc. of DesignCon 2006, Jan.31-Feb.3 2006, Santa Clara, CA.
[4] Scott McMorrow, Chris Heard, “The Impact of PCB Laminate Weave on the Electrical Performance of Differential Signaling at Multi-Gigabit Data Rates”, Proc. of DesignCon 2005, Jan. 31-Feb. 3, Santa Clara, CA.
[5] Clayton R. Paul, “Analysis of Multiconductor Transmission Lines”, Wiley Series on Microwave and Optical Engineering.